

# *Supporting Information*

## **Validation of an electronic VOC sensor against gas chromatography**

Xiao Zhu,<sup>1,2</sup> Waqar Ahmed,<sup>3</sup> Kamila Schmidt,<sup>3</sup> Stephen J. Fowler,<sup>3</sup> Christopher F. Blanford<sup>1,2,\*</sup>

<sup>1</sup> Department of Materials, University of Manchester, Oxford Road, Manchester, M13 9PL, UK

<sup>2</sup> Manchester Institute of Biotechnology, University of Manchester, 131 Princess Street, Manchester, M1 7DN, UK

<sup>3</sup> Division of Infection, Immunity and Respiratory Medicine, University of Manchester, Oxford Road, Manchester, M13 9PL, UK

*Email: christopher.blanford@manchester.ac.uk*

<b>Gas sampling system.....</b>	<b>S-2</b>
<b>Gas control system .....</b>	<b>S-3</b>
<b>BME680 gas sensor specifications and format .....</b>	<b>S-4</b>
<b>Qualitative flow rate test .....</b>	<b>S-6</b>
<b>Mass spectrum.....</b>	<b>S-7</b>
<b>Quantitative data analysis of BME680 sensor calibration .....</b>	<b>S-8</b>
<b>Quantitative data analysis of TD-GC-MS calibration.....</b>	<b>S-10</b>
<b>Representative responses for BME680/GC validation studies .....</b>	<b>S-11</b>
<b>Variation in sensor response .....</b>	<b>S-15</b>
<b>Calibration protocol.....</b>	<b>S-17</b>
<b>Additional micrographs of BME680 gas sensor.....</b>	<b>S-18</b>
<b>Comparison of electronic and TD-GC-MS VOC sensing .....</b>	<b>S-19</b>

Published article on IEEE Xplore: <https://doi.org/10.1109/TIM.2024.3485428>

Repository on FigShare: <https://doi.org/10.48420/c.7294807>

## Gas sampling system

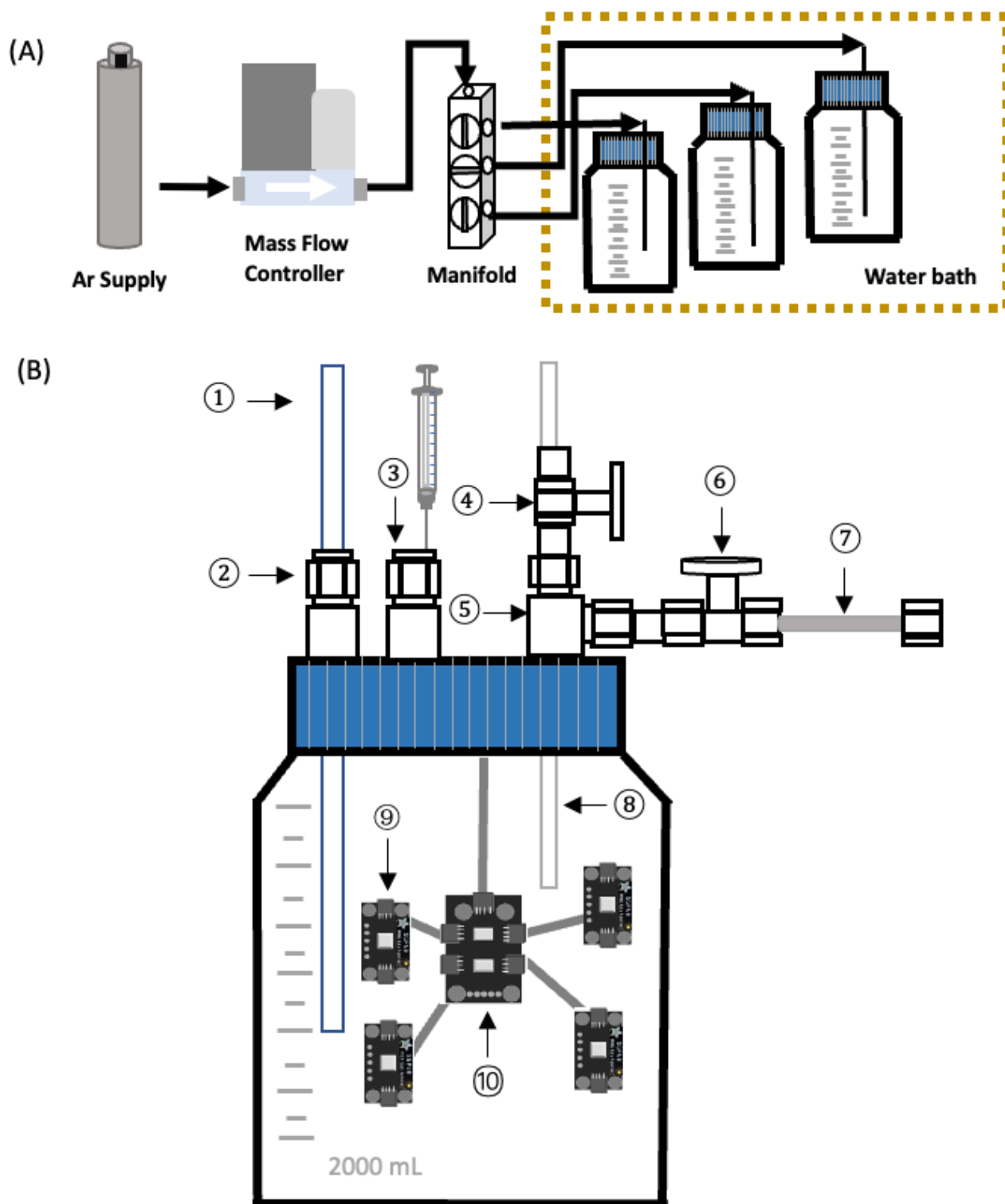


**Fig. S1. Schematic of the gas sampling system.** (A) Argon enters through a mass-flow controller (MFC) and then is split using a metal manifold to enter a temperature-controlled bath containing 2L gas-sampling bottles. (B) Diagram of the connections to the gas sampling bottle. ① polyurethane tube ② stainless steel union ③ septum ④ stainless steel ball valve ⑤ stainless steel three ways tee valve ⑥ stainless steel needle valve ⑦ Tenax TA tube ⑧ 316 stainless steel tube ⑨ BME680 sensor ⑩ multiplexer.

## Gas control system

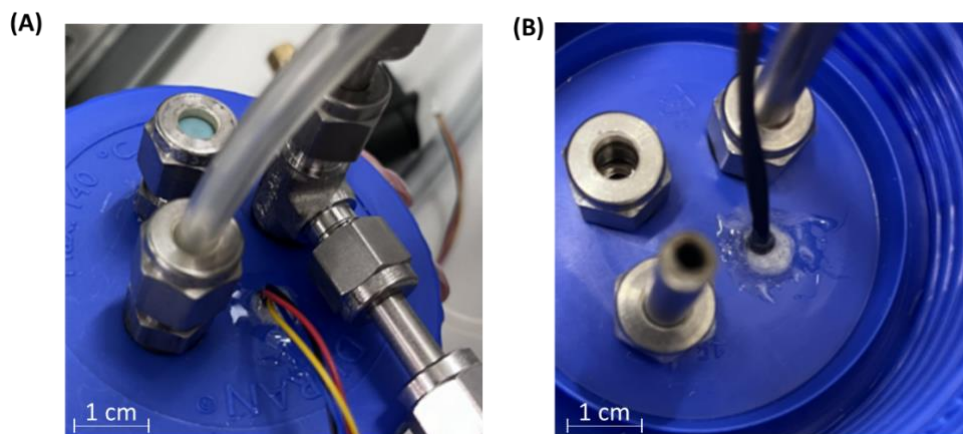


**Fig. S2.** The linking point of the QT/QWIIC JST cable goes through the lid of the Duran bottle. The cable passed through the drilled hole on the lid, then the hole was filled with cotton wool and covered by epoxy glue. (A) The outside of the lid. (B) The inside of the lid.

**BME680 gas sensor specifications and format**

The electronic BME680 sensor and Raspberry Pi were connected via a custom-built system using commercially available components (Fig. S4). The hardware included a PCA9546 4-channel STEMMA QT/QWIIC I2C multiplexer (Adafruit 5664) or a TCA9548A 1-to-8 I2C multiplexer (Adafruit 2717) linked to a Raspberry Pi 3B+ Model B single-board computer via a half-size breadboard. The BME680 breakouts inside the glass bottles were connected using STEMMA QT/QWIIC JST cables along with the LTC4311 I2C extenders (Adafruit 4756). To create an airtight environment within the glass bottle, the QT/QWIIC JST cable connecting to the BME680 sensor was threaded through the drilled hole on the lid, which was then sealed with cotton wool to occupy the rest of the space. (Fig. S2) A 2-part epoxy (Gorilla 6044000) was used to cover and secure the cable and wool through the hole.

**Table SI. Selected specifications for the BME680<sup>a</sup>**

<b>Gas sensor response time (<math>\tau_{33-63\%}</math>)</b>	< 1 s (for new sensors)
<b>Gas sensor sensor-to-sensor deviation</b>	$\pm 15\%$
<b>Humidity sensor response time (<math>\tau_{0-63\%}</math>)</b>	8 s
<b>Humidity sensor accuracy tolerance</b>	$\pm 3\%$ RH
<b>Humidity sensor hysteresis</b>	$\leq 1.5\%$ RH
<b>Pressure sensor RMS Noise</b>	0.12 Pa
<b>Pressure sensor sensitivity error</b>	$\pm 0.25\%$
<b>Pressure sensor temperature coefficient offset</b>	$\pm 1.3$ Pa/K

<sup>a</sup> Source: <https://www.bosch-sensortec.com/products/environmental-sensors/gas-sensors/bme680/> accessed 2023-12-06

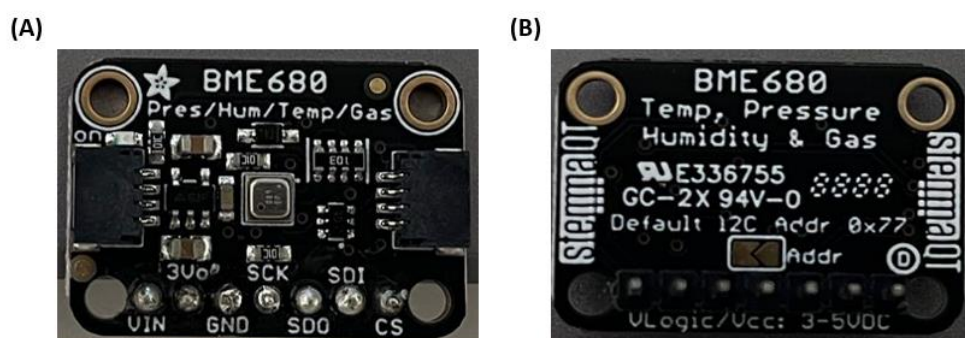


**Fig. S3. BME680 breakout board with I<sup>2</sup>C and SPI interfaces (Adafruit 3660). (A) Top of the breakout. The sensor is the 3.0 mm × 3.0 mm × 0.93 mm metal device in the center of the board. The black connectors on the left and right are STEMMA/QT (4-pin JST PH) connectors for I<sup>2</sup>C communication. (B) bottom side of the sensor.**

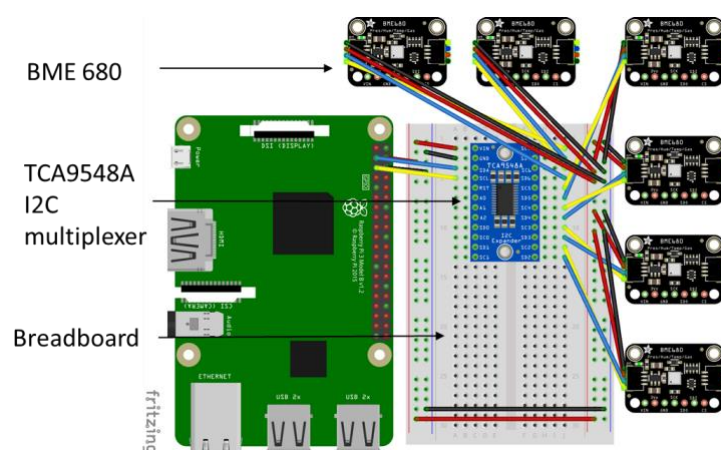


**Fig. S4. Fritzing diagram of the connections between the Raspberry Pi sampling system and the BME680 sensor breakouts.**

### Qualitative flow rate test

The performance of the gas control system was tested by a dry ice test. It is fast, easy to conduct, cheap, reproducible, noncontaminating of the environment, and a reliable indicator of the control system gas circulate performance. The flow rate test can be used to verify that the chamber will contain and mix chemical vapors under actual conditions at various flow rates.[1] The term 'smoke' as used below refers to the mixture of carbon dioxide vapor and water droplets resulting from dry ice (solid carbon dioxide) and liquid water in the glass bottle.

At the beginning, three times, fold blue rolls were put in the gas control system, the blue roll was covered with 100 g of dry ice and 30 mL of tap water was added. The lid was closed immediately, and the gas inlet was switched on. If the smoke in the bottle gradually becomes clearer or forms a swirling flow, and the laser can go through the smoke, the mixture ability of the flow rate is enough to mix the VOC gas in the bottle. If part of the smoke settles to the bottom, only the top part becomes clearer. Also, the laser scattered by the gas cannot pass through the smoke, and the flow rate will not be able to mix the gas evenly. The tested flow rate includes 50, 100, 200, 400, 1000 sccm. At a flow rate of 50 sccm, the gas on top turned to clear first, and part of the smoke settled down to the bottom (Fig. S5(B)), indicating the flow rate cannot mix the gas well. From 100 to 800 sccm flow rate, the gas in the bottle turned to clear gradually (Fig. S5(A)), and the speed increased with the increasing flow rate from 30 seconds to 9 seconds. In conclusion, the flow rate of 100 sccm is enough to mix the gas evenly.

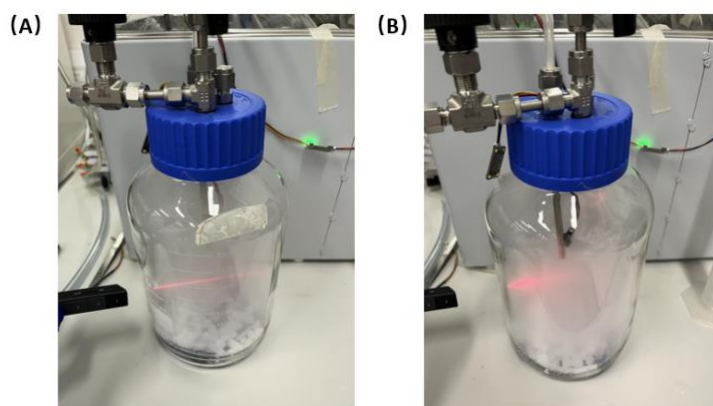


**Fig. S5. (A) Gas mixed evenly in the gas control system. The laser light can go through the smoke. (B) Gas settled down to the bottom of the gas control system. The laser light cannot go through the smoke.**

- [1] J. B. Adams, "Synthesis-laboratory fumehoods: Easy, reliable performance evaluation and importance of sash design," *Journal of Chemical Education*, vol. 66, no. 12, Dec. 1989, doi: 10.1021/ed066pa289.

## Mass spectrum

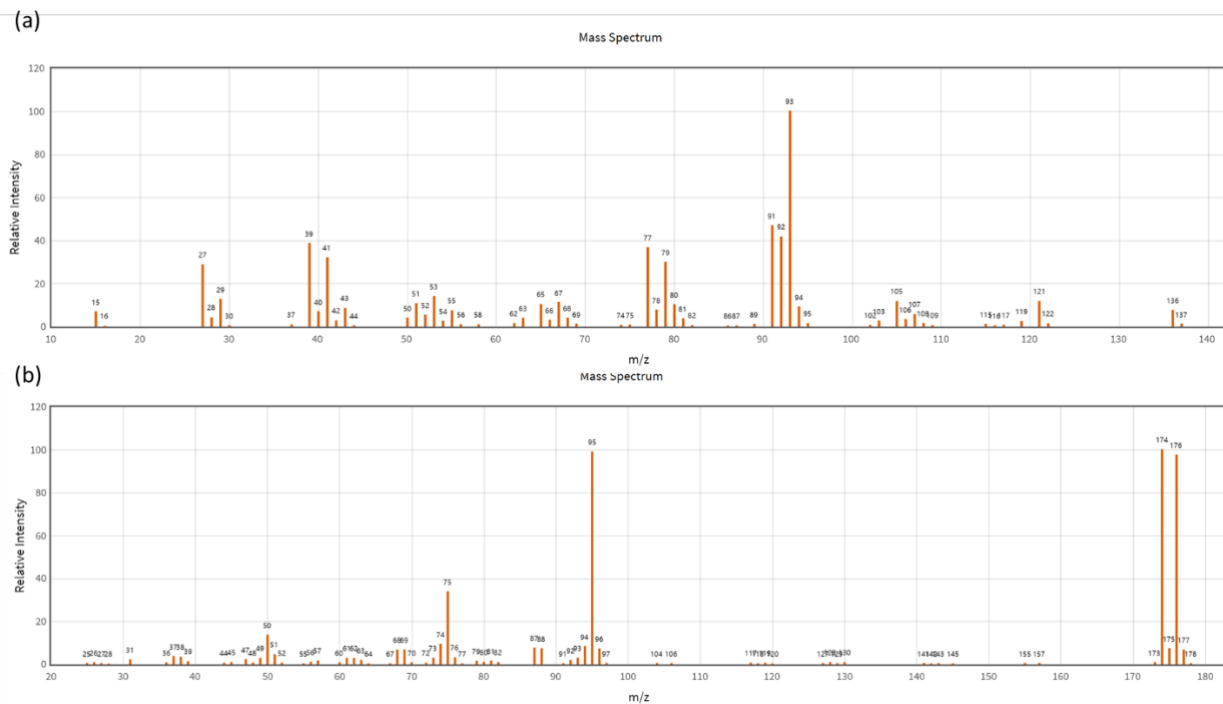


**Fig. S6.** EI 70 eV spectra of (a)  $\alpha$ -pinene. (b) 4-bromofluorobenzene.

Source:

- (a) <https://webbook.nist.gov/cgi/cbook.cgi?ID=C80568&Mask=200>,
- (b) <https://webbook.nist.gov/cgi/inchi?ID=C460004&Mask=200>, accessed 2024-03-14

Quantitative data analysis of BME680 sensor calibration

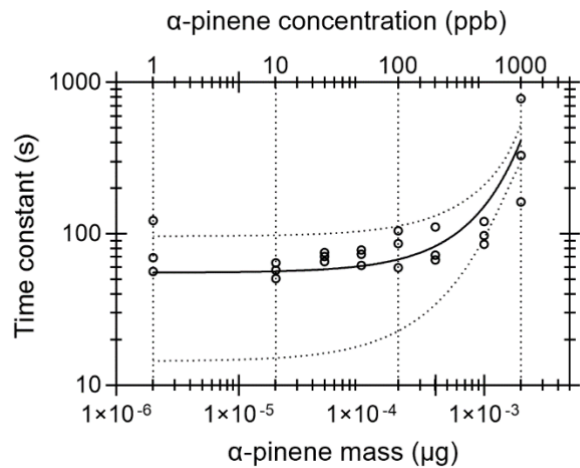


**Fig. S7.** Log-log plot of the time constant against the mass of  $\alpha$ -pinene at the third reaction peak with three repetitions. Each shape (square, circle, triangle) represents one repetition. Time constants were calculated by first-order fitting. The solid line represents an exponential fit to the data. The dashed lines represent the 95 % CI for the fit.

**Table SII.** Sensitivity and limit of detection for three BME680 sensors. Values for uncertainty are from the standard error of the first-order polynomial fit.

Sensitivity (R %/ppb)	LOD (ppb)
$0.063 \pm 0.02$	20.11
$0.081 \pm 0.01$	25.61
$0.064 \pm 0.02$	38.96

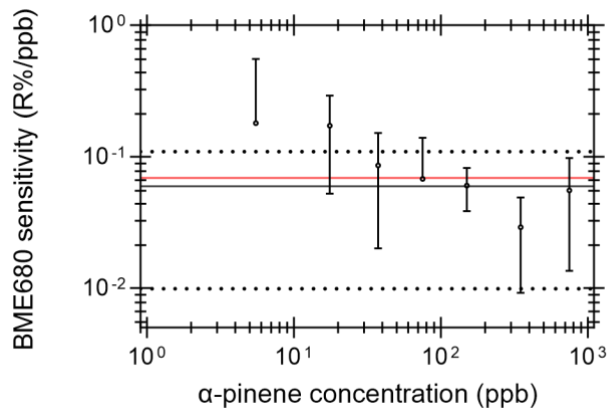


**Fig. S8.** Log-log plot to show the linear range of the BME680 sensor. The derivative is based on the slope against concentrations of  $\alpha$ -pinene. The error bar represents the mean  $\pm$  SD of three independent measurements. The red line is the slope of the linear fitting of response ratios versus all concentrations (Fig. 1(B)), while the black line is the mean value of sensitivity above 37 ppb. The band between two black dots lines is the  $\pm 95\%$  CI of the mean value of sensitivity above 37 ppb.



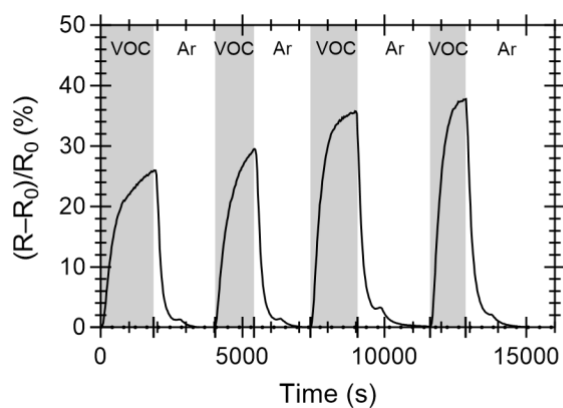


**Fig. S9. Four repetitions of the 1000 ppb  $\alpha$ -pinene calibration test. The grey areas depict the gas static time ( $\alpha$ -pinene released within the bottle), while the white areas reflect the argon purging time at a flow rate of 800 sccm.**

### Quantitative data analysis of TD-GC-MS calibration

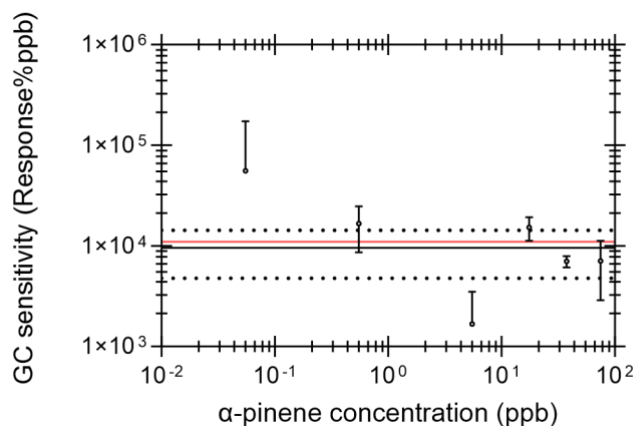


**Fig. S10.** Log-log plot showing the linear range of the TD-GC-MS. The derivative is based on the slope against concentrations of  $\alpha$ -pinene. The error bar represents the mean  $\pm$  SD of three independent measurements. The red line is the slope of the linear fitting of response ratios versus all concentrations (Fig. 1(E)), while the black line is the mean value of sensitivity above 0.55 ppb. The band between two black dots lines is the  $\pm 95\%$  CI of the mean value of sensitivity above 0.55 ppb.

### Representative responses for BME680/GC validation studies

Fig. S11(A) shows a sample BME680 response to 100 ppb  $\alpha$ -pinene. The dark blue areas are the  $\alpha$ -pinene releasement within the gas control system, while the white areas are the duration of argon purging at a flow rate of 800 sccm and water bath temperature at  $(25.4 \pm 0.4) ^\circ\text{C}$ . To be consistent with the calibration test and to allow the volatile gas to be fully released, the sample was collected in the third replicate. The black dotted circle indicates the fluctuation in the response when the microsyringe extracts volatile gas from the septa for GC analysis.

The different tested concentration reaction curves have been presented in Fig. S11(B). Similarly, the response curves from different concentrations showed some variation in extracting volatile points. This real-time dynamic changed graph provided helpful information in the practical application. In addition, the slope trend of the response curve is consistent with the calibration test. The higher the concentration, the steeper the slope of the curve and the harder it is to reach equilibrium.

The chromatograms from GC have been plotted in Fig. S11(C). The retention time of the  $\alpha$ -pinene ion ( $m/z$  93) was changed from 3.09 minutes in calibration tests to 3.12 minutes in validation tests. The possible reasons are the column in the GC was trimmed, the transfer line in GC was replaced during regular maintenance, and the usage degree of different TA tubes also affects the retention time.

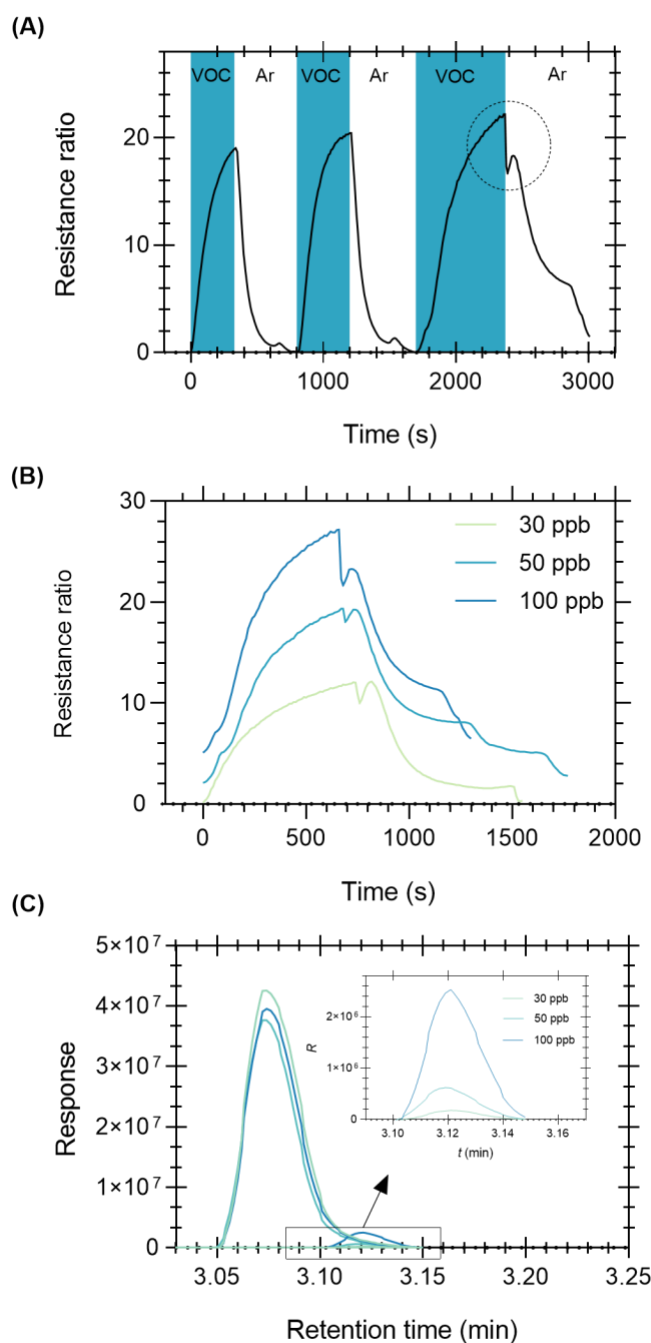


**Fig. S11. Validation between BME680 sensor and TD-GC-MS. (A)** A complete releasement of 100 ppb  $\alpha$ -pinene occurred in the gas control system. The blue regions depict the  $\alpha$ -pinene released within the bottle, while the white regions show the duration of argon purging at a flow rate of 800 sccm and a bath temperature of  $(25.4 \pm 0.4) ^\circ\text{C}$ . The dotted circle denotes the gas collection point by a gastight microsyringe. **(B)** The third peaks result from three repetitions of 20 ppb, 50 ppb and 100 ppb  $\alpha$ -pinene. The irregular curves are the collection point. The offset of the 50 ppb line is  $y=2$  data units, and the 100 ppb line is  $y=5$  data units, and the total units is 30. **(C)** Chromatograms of ISTD and  $\alpha$ -pinene ion ( $m/x$  77). The inset depicts the consistently increasing response from increasing  $\alpha$ -pinene concentration.

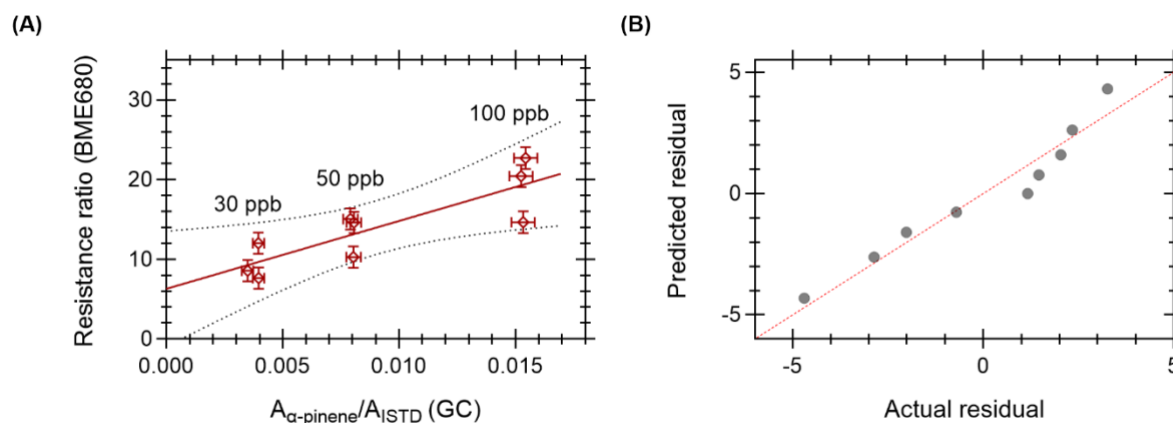


**Fig. S12. Validation of single BME680 sensor against TD-GC-MS for  $\alpha$ -pinene.** The red horizontal error bars represent the propagated uncertainty of the relative response for the GC and the vertical error bars represent the propagation uncertainty of the relative response for the BME680 sensor. The red line connected to three dots represents the linear regression curve, and the black dotted curve line represents the 95 % confidence interval for the fit. Each concentration has three repetitions. (B) Normal Quantile-Quantile plot comparing the distribution of measurement from BME680 gas sensor to GC method. The red line is a reference line, representing the two sets of data have the same distribution.

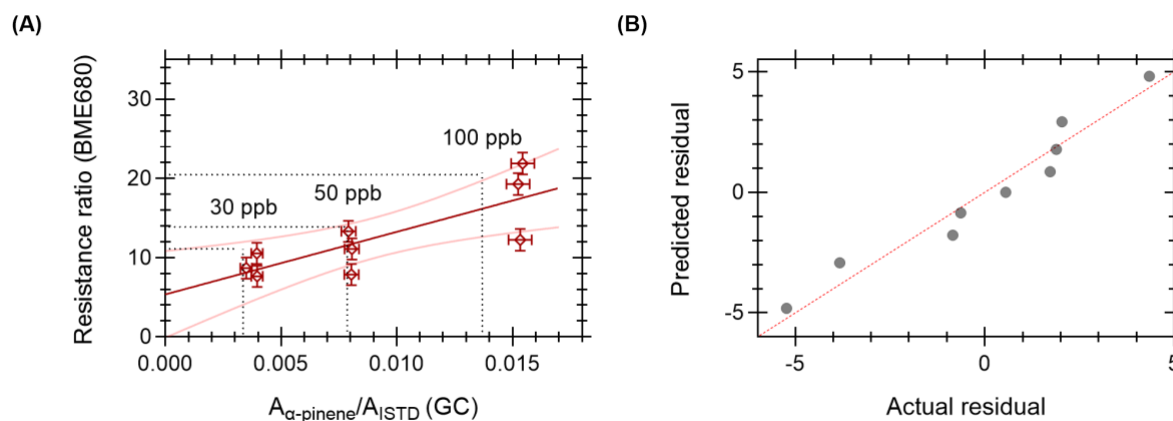


**Fig. S13. Validation of single BME680 sensor against TD-GC-MS for  $\alpha$ -pinene.** The red horizontal error bars represent the propagated uncertainty of the relative response for the GC and the vertical error bars represent the propagation uncertainty of the relative response for the BME680 sensor. The red line connected to three dots represents the linear regression curve, and the black dotted curve line represents the 95 % confidence interval for the fit. Each concentration has three repetitions. (B) Normal quantile-quantile plot comparing the distribution of measurement from BME680 gas sensor to GC method. The red line is a reference line, representing the two sets of data have the same distribution.

**Variation in sensor response**

The resistance data shown in Fig.3 was fit to a first-order kinetic model, the values of  $R_0$ ,  $\Delta R$ , and time constant ( $\tau$ ) from three injections for each sensor are shown in Table SIII, indicating the variation across sensors.

**Table SIII. Parameters from a first order fit to the VOC equilibration responses are shown in Fig. 3(A) (200 ppb  $\alpha$ -pinene in static argon).**

Sensor no.	Parameter	Injection 1	Injection 2	Injection 3
0	$\tau$ (s)	132.10	78.92	100.90
1	$\tau$ (s)	139.40	92.45	115.80
2	$\tau$ (s)	176.20	113.90	145.30
3	$\tau$ (s)	160.80	96.34	120.30

**Table SIV. Sample correlation matrix comparing the response between four sensors recording three exposures to 200 ppb  $\alpha$ -pinene in static argon. Fig. 3(C)**

Sensor no.	0	1	2	3
0	1.000	0.962	0.964	0.979
1	0.962	1.000	0.948	0.989
2	0.964	0.948	1.000	0.981
3	0.979	0.989	0.981	1.000

**Table SV. Relative variation in the responses between four sensors to six concentrations of  $\alpha$ -pinene before and after calibrations. Fig. S14**

concentration (ppb)	no calibration	one-point calibration	two-point calibration
25	30.8 %	30.4 %	5.4 %
50	25.5 %	22.9 %	5.0 %
100	33.5 %	30.8 %	5.7 %
200	23.6 %	20.0 %	6.9 %
500	34.7 %	31.8 %	5.9 %
1000	30.2 %	28.5 %	5.8 %

Table SIV summarizes the metric used to calculate standardized error before and after calibrations, which is given by equation S1.

$$\varepsilon = \sqrt{\frac{1}{N \cdot Z(\bar{S})} \sum_{i=0}^N \text{var}(S(t_i))} \quad (\text{S1})$$

where  $N$  is the number of time points,  $i$  is the time point index,  $\text{var}(S(t_i))$  is the variance of the sensor response at time point  $i$ , and  $Z(\bar{S})$  is the range of the mean sensor response over all time points. The sample variance in the response for a single time point is calculated in the standard way (equation S2).

$$\text{var}(S(t_i)) = \frac{\sum_{j=0}^M (s(t_i^j) - \bar{s}(t_i))^2}{M} \quad (\text{S2})$$

where  $M$  is the number of sensors,  $j$  is the sensor index,  $S_i^j$  is the response of sensor  $j$  at time point  $t_i$ , and  $\bar{S}(t_i)$  is the mean sensor response at time point  $t_i$ .

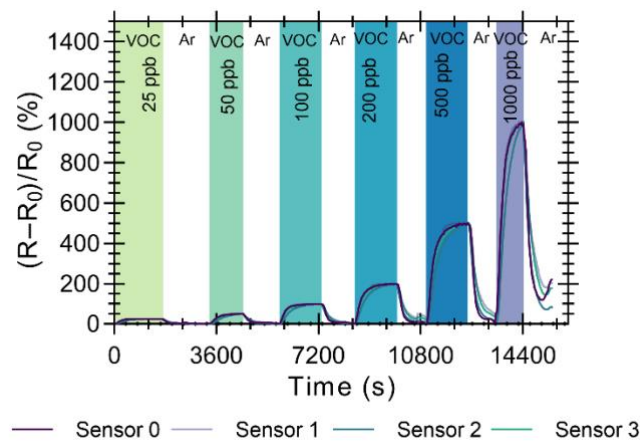


**Fig. S14. Calibrated peaks of BME680 sensor response to the static concentrations of pinene (colored regions) alternating argon purging at 800 sccm.**

To further demonstrate the calibration protocol, the calibration method was applied to the data from continuously running tests. Five different concentrations from 50 to 1000 ppb of  $\alpha$ -pinene were sequentially injected into the gas sampling system without interruption. Each concentration was injected three times to achieve a stable third peak. A sample correlation matrix is given in Table SVI. The correlation coefficient between the sensors ranged from 0.95 to 0.99. Consistent with the highly correlated responses, two-point calibration reduced the response variation between sensors to 5–7 % (Table SVII).

**Table SVI. Sample correlation matrix comparing the response between four sensors recording three exposures to 200 ppb  $\alpha$ -pinene in static argon for continuously acquired data.**

Sensor no.	0	1	2	3
0	1.000	0.977	0.962	0.989
1	0.977	1.000	0.942	0.988
2	0.962	0.942	1.000	0.977
3	0.989	0.988	0.977	1.000

**Table SVII. Relative variation in the responses between four sensors to six concentrations of  $\alpha$ -pinene before and after calibrations for continuously acquired data.**

concentration (ppb)	no calibration	one-point calibration	two-point calibration
50	39.4 %	22.2 %	5.7 %
100	31.4 %	18.8 %	6.7 %
200	29.7 %	20.0 %	6.8 %
500	38.0 %	20.5 %	7.8 %
1000	39.8 %	22.2 %	7.1 %



### Calibration protocol

After two-point calibration, the concentration of volatile ( $c$ ) measured by a calibrated BME680 sensor is given by equation S3.

$$c = F \left( \frac{R - R_0}{R_0} \right) \quad (\text{S3})$$

where  $R$  is the measured resistance  $R_0$  is the sensor's resistance in the absence of volatile (in this case, argon only) and  $F$  is a calibration constant calculated by equation S4.

$$F = \frac{c_{\text{calib}} R_{\text{calib}}}{R_{\text{calib}} - R_0} \quad (\text{S4})$$

where  $R_{\text{calib}}$  is the sensor's response in the presence of a known concentration ( $c_{\text{calib}}$ ) of volatile in the same atmosphere.

## Additional micrographs of BME680 gas sensor

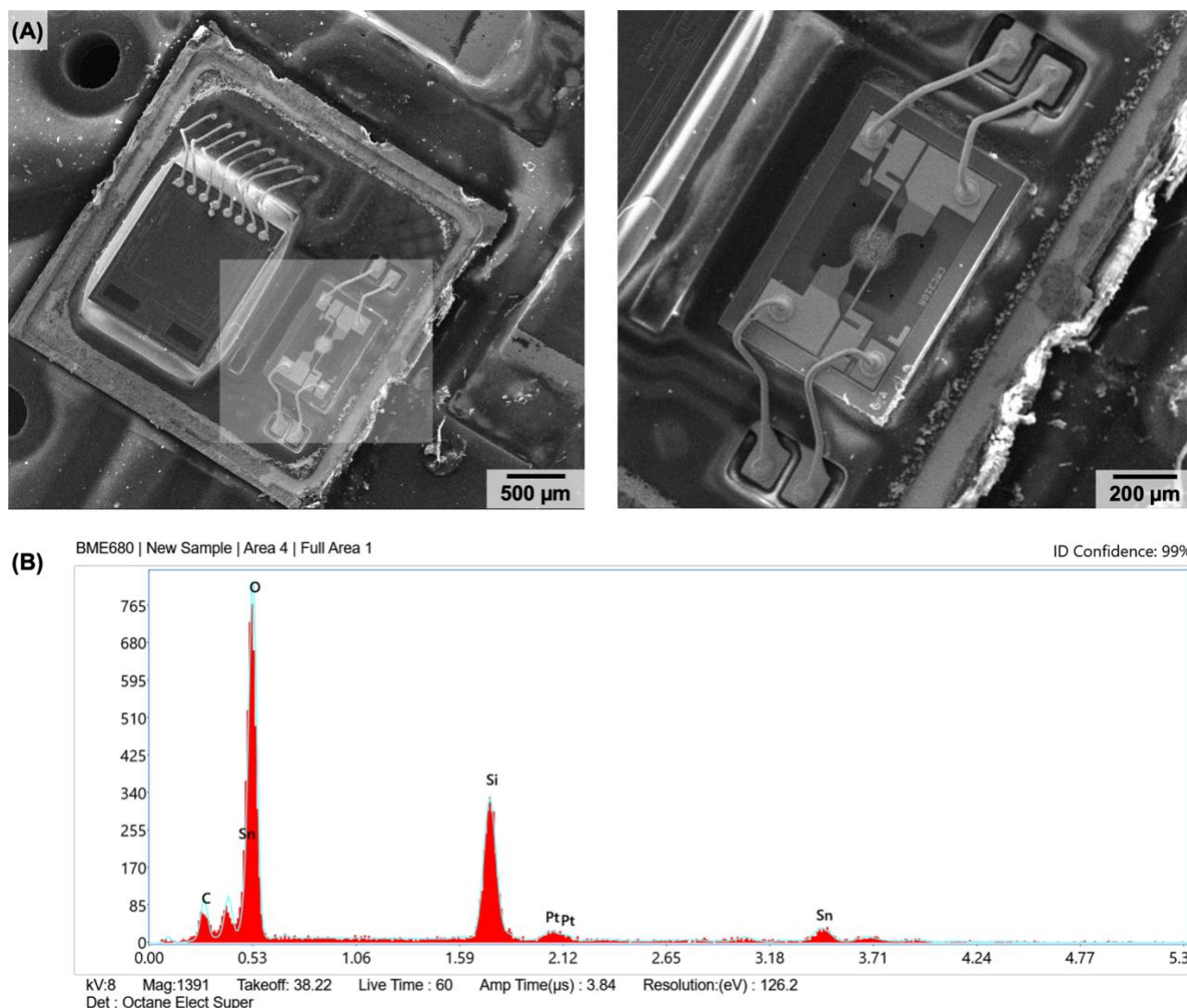


**Fig. S15. (A) Scanning electron microscope (SEM) images of the gas sensing region of a BME680 gas sensor. The translucent white square on the left-hand image corresponds to the area shown in the right-hand image. (B) Energy-dispersive X-ray spectrum taken of the area shown in Fig. 4. The  $x$ -axis gives the X-ray energy in keV and the  $y$ -axis gives the number of counts for a given X-ray energy.**

## Comparison of electronic and TD-GC-MS VOC sensing

**Table SIV. Pros and cons of the BME680 gas sensor and TD-GC-MS. Stars indicate which method has the more desirable value.**

Factor	TD-GC-MS	BME680 gas sensor
Sampling time	1 min. ★	~5 min.
LoD ( $\alpha$ -pinene)	~1 ppb ★	~30 ppb
Response ( $\alpha$ -pinene)	~1 % L $\mu\text{g}^{-1}$ ★	~30 % L $\text{mg}^{-1}$
Output frequency	~2 h <sup>-1</sup>	~1 s <sup>-1</sup> ★
Repeatability (CoV)	~4 % ★	~3 %
Equipment	~£150,000	~£100 ★
Maintenance/operation	~£1000	~£10 ★
Selectivity	physically (GC and MS) ★	algorithmically
Visualization	fragment count vs. retention time	gas resistance vs. time